

Probability Distribution Functions for Transmission of Waves through Random Media: A New Numerical Method

I. Edrei and M. Kaveh

Department of Physics, Bar-Ilan University, Ramat-Gan 52100, Israel

B. Shapiro

Department of Physics, Technion, Haifa, Israel

(Received 19 August 1988; revised manuscript received 24 February 1989)

We present a new numerical method for calculating interference phenomena for waves propagating through random media. The model is applied to calculate probability distribution functions for the transmission $P(T)$ in one and two dimensions, T being the transmission coefficient. The model reproduces the analytical predictions for one dimension, and yields new results for two-dimensional systems. The distribution function $P(T)$ in two dimensions, in the diffusive regime, is found to be close to a Gaussian with a variance proportional to the mean, in agreement with the results of diagrammatic calculations. A crossover of the distribution to log-normal behavior typical for strong localization is obtained.

PACS numbers: 42.20.-y

In recent years there has been a renewed interest in wave propagation (electron waves,¹ electromagnetic waves,² and acoustical waves³) through random media. It is now understood that interference between multiply scattered waves leads to unusual phenomena, such as universal conductance fluctuations in weakly disordered metals.⁴⁻⁶ These fluctuations have been observed⁷ in mesoscopic structures,⁸ i.e., when the sample size was smaller than the inelastic scattering length (the length that an electron travels between two inelastic collisions). For optical waves, the inelastic length is macroscopic and intensity fluctuations (speckle) patterns were recently observed⁹ and interpreted as being due to interference phenomena caused by multiple scattering.¹⁰ For these systems, it was recently predicted^{11,12} that there would be anomalously large fluctuations in the transmission coefficient for optical waves. This implies that in disordered systems, it is not sufficient to consider only averaged values of a physical quantity but one must examine the full probability distribution.

In this Letter, we present a new numerical method for studying interference phenomena and fluctuation effects. We have obtained the full probability distribution function $P_L(T)$, where T is the transmission coefficient for a slab of thickness L and width W . We find that for $W \gg L$, this function is quite accurately represented by a Gaussian. We hope that this prediction will encourage measurements of distribution functions for the transmission coefficients for optical waves. We have also studied the strip geometry, $W \ll L$, and find a crossover in the distribution function as L increases. We have also checked the reliability of our new method by calculating $P_L(T)$ for a one-dimensional system. Our probability distribution function is in excellent agreement with analytical predictions in both the weak- and strong-disorder limits. Finally, our method yields new results for the variance of the transmission coefficient for a

two-dimensional system, in agreement with the theory of Stephen and Cwilich¹¹ and Feng *et al.*¹² when applied to two dimensions.

Our method is quite general, and thus is appropriate for studying interference phenomena either for electron waves (which obey the Schrödinger equation) or for electromagnetic waves (which obey Maxwell's equations). The new insight here is that at each step of the calculation we deal only with a *local* scattering event (single-scattering process). The interference due to multiple scattering is built up in time until the steady state is achieved.

We first describe our numerical method and then discuss the results that we obtained for the distribution function of the transmission coefficient. We consider a set of complex numbers $\psi_a(m)$ which define the wave function (or the electric field for optical waves) at a discrete time m . The index a may refer, for example, to sites on a lattice. At the next instant, $m+1$, the wave function is determined by

$$\psi_a(m+1) = \sum_{\beta} G_{a\beta} \psi_{\beta}(m). \quad (1)$$

The matrix $G_{a\beta}$ (the Green's function) is a unitary matrix. It should also obey other symmetries of the problem, such as the time-reversal symmetry (if present). We assume that $G_{a\beta}$ is independent of m , which corresponds to a time-independent potential (quenched disorder).

Let us now be more specific and imagine a lattice of blocks (sites) and pipes (bonds) such as illustrated in Fig. 1. Each site represents a scatterer and is described by a $2D \times 2D$ scattering S matrix, D being the dimensionality (one can also allow for "empty" sites by assigning to them a unit S matrix).¹³ The bonds represent free propagation between the blocks. The wave function $\psi_a(m)$ is defined by a set of $2N_b$ amplitudes (a

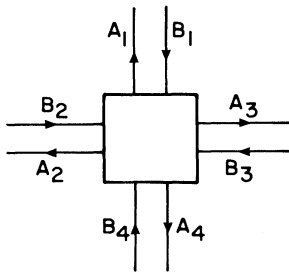


FIG. 1. The block represents a two-dimensional scatterer. A and B are the outgoing and ingoing amplitudes, respectively. They are related by the equation $A_i = \sum_{j=1}^4 S_{ij} B_j$, where S_{ij} is the 4×4 scattering matrix for the scatterer.

$= 1, 2, \dots, 2N_b$), where N_b is the number of bonds in the lattice and each bond carries two waves propagating in opposite directions. An S matrix at each site transforms the 2D incoming amplitudes (at time m) into 2D outgoing amplitudes (at time $m+1$). Thus, the stationary solution is built up step by step in time, eliminating the need to diagonalize a very large $2N_b \times 2N_b$ matrix. To specify the model completely, we need to define the S matrix assigned to each block. It is convenient also to include in the S matrix the free propagation in the bond, so that each block includes its corresponding half bonds. The phases for each bond (see Fig. 1) are denoted by ϕ_i ($i=1, 2, \dots, N_b$). We confine ourselves to isotropic scatterers and assume time-reversal symmetry. The S matrix is then defined by four complex numbers which correspond to scattering in four directions (forward transmission t , reflection r , scattering to the right r_R , and scattering to the left r_L). This is specified as $t = |t| e^{i\phi_t}$, $r = |r| e^{i\phi_r}$, and $r_L = r_R = |r_L| e^{i\phi_L}$.

The scattering complex amplitudes, t , r , and r_L , are chosen to be the same for all the scatterers. The phases ϕ_i on the bonds are changed from bond to bond independently according to a uniform distribution between 0 and 2π . This corresponds to a specific model of identical scatterers separated by distances (bonds) which are distributed between some distance a and $a+\lambda$ (where λ is the wavelength). However, studies of various models¹³⁻¹⁶ suggest that, for weak disorder, the specific type of randomness is of no importance: The randomness enters only via a single parameter—the measure of local disorder. Thus, other kinds of randomness could be chosen. This particular choice is motivated by the recent successful real-space theories¹⁴ for calculating correlation functions by following multiple-scattering Feynman paths with random phases at each step. The unitary and symmetric S matrix for the object in Fig. 1 is defined as

$$S_{lm} = a_{lm} \exp[i(\phi_l + \phi_m)], \quad (2)$$

where $a_{11} = r$, $a_{12} = a_{13} = a_{24} = a_{34} = r_L$, and $a_{14} = a_{23} = t$ for $l, m = 1, \dots, 4$ with the following constraint (for the

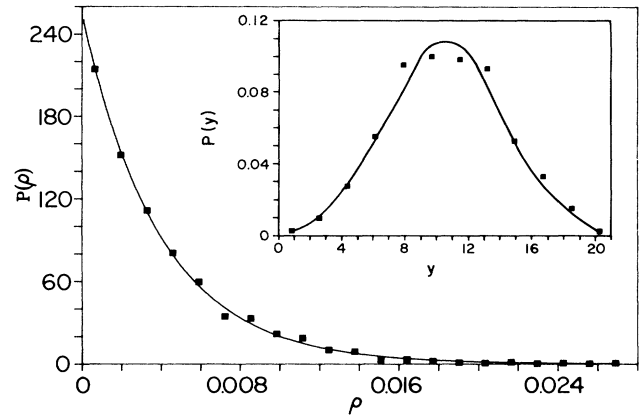


FIG. 2. Resistance distribution for a one-dimensional chain of forty scatterers. The squares represent the numerical simulation and the solid curve represents the Poisson distribution with $\bar{\rho} = 0.004$. Inset: A plot of $P_L(\ln T)$ as a function of $\ln T$ for $L=40$ and $\rho_0 = \frac{1}{3}$. The solid curve is the theoretical Gaussian distribution.

choice $\phi_L = 0$):

$$tg\phi_t = (|t| + |r| \cos\phi_0) / |r| \sin\phi_0, \quad (3)$$

where

$$\phi_0 = \phi_r - \phi_t = \cos^{-1}(-|r_L|^2 / |r| |t|)$$

and

$$|r|^2 + 2|r_L|^2 + |t|^2 = 1.$$

It is easy to show that the unitarity of the individual S matrix ensures the unitarity of the matrix $G_{\alpha\beta}$ for the entire sample. We first demonstrate that the above model, when applied to a disordered one-dimensional system, yields results in excellent agreement with analytical predictions. In one dimension, of course, $r_L = 0$.

Let us consider weak disorder, i.e., the resistance $\rho_0 \equiv |r|^2 / |t|^2$ of each scatterer is small. It is known^{15,16} that as long as the length of the chain L is much smaller than the localization length $\xi \equiv a/\rho_0$ (but larger than the distance a between scatterers), the distribution $P_L(\rho)$ for the total resistance $\rho \equiv R/T$ (R and T are the reflection and transmission coefficients for a chain of length L) is given by

$$P_L(\rho) = \bar{\rho}^{-1} \exp(-\rho/\bar{\rho}), \quad (4)$$

where $\bar{\rho} = \rho_0 L$. In Fig. 2, we compare with Eq. (4) our numerical results obtained for $L=40$ and $\rho_0 = 10^{-4}$ for an ensemble of 2000 realizations. The agreement is very good. We have also verified for $L=40$ and $\rho_0 = \frac{1}{3}$ (see the inset of Fig. 2) which corresponds to the strong-disorder case, that $P_L(\ln T)$ exhibits a Gaussian distribution in agreement with theory (see, e.g., Refs. 15 and 16 where references to earlier work were given).

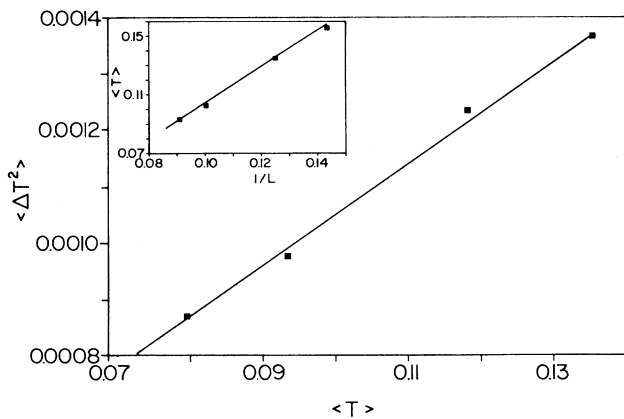


FIG. 3. The squares represent the variance of T vs $\langle T \rangle$ for a slab with $W=50$ and $L=7, 8, 10,$ and 11 . Inset: $\langle T \rangle$ as a function of $1/L$.

We now extend our model to two-dimensional systems of different geometries and find entirely different results. We consider the case where the disorder is due to the random phases ϕ_i on each bond. The strength of each scatterer is assumed to be the same and provides the measure of the local disorder (which determines the mean free path). We choose symmetric scatterers, i.e., $|r| = |r_L| = |t|$ which, by the unitarity relations, implies $|r|^2 = 0.25$. (As will be shown below, this local disorder is weak in the sense that a diffusive regime exists; i.e., intensity propagates basically by a classical diffusion process, which implies that the wavelength λ is much shorter than the elastic mean free path l .) First, we consider a slab of thickness L and width W . The width W is illuminated by a plane wave, and reflecting boundary conditions are applied on the sides perpendicular to the direction of propagation. This corresponds to a wave incoming in one channel (channel a) which is reflected or transmitted into all other channels b . The total transmission T_a is given by the sum over all the outgoing channels, $T_a = \sum T_{ab}$, where T_{ab} is the transmission coefficient from a to b . According to the diagrammatic calculations,^{11,12} in the diffusive regime (where $l \gg \lambda$), $\langle T \rangle \approx l/L$ and $\langle \Delta T^2 \rangle \approx (\alpha/N)\langle T \rangle$, where N is the number of channels and α is a dimensionless number of order unity^{11,12} (for brevity, we have suppressed the index a in the transmission).

We have calculated the probability distribution $P_L(T)$ for four different values of L ($L=7, 8, 10,$ and 11) with a fixed value of $W=50$ and constant disorder. Let us first discuss the behavior of $\langle T \rangle$ and $\langle \Delta T^2 \rangle$. These quantities are plotted in Fig. 3 where the four squares represent the results for four different lengths. To a good approximation, these squares fall on the straight line in agreement with the theoretical prediction $\langle \Delta T^2 \rangle \propto \langle T \rangle$. In the inset of Fig. 3, we plot $\langle T \rangle$ as a function of $1/L$ and the straight line obtained indicates that we are in the

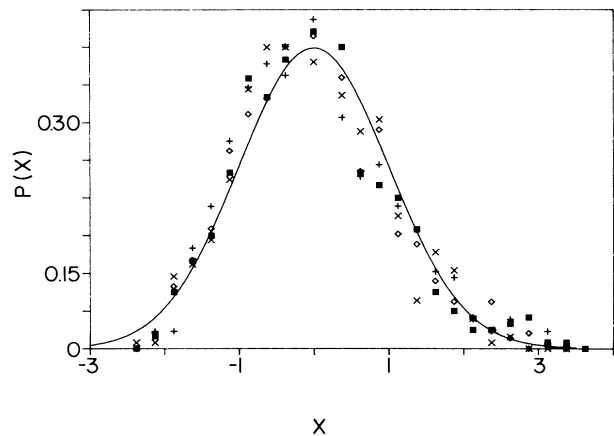


FIG. 4. The four distribution functions for the four values of L (see text). The symbols $\blacksquare, \times, \diamond,$ and $+$ correspond to $W=50$ and $L=7, 8, 10,$ and 11 , respectively. The solid curve represents the Gaussian function $(2\pi)^{-1/2} \exp(-X^2/2)$.

diffusive limit appropriate to weak disorder (namely, $L \ll \xi$, where ξ is the localization length).

Next, let us consider the full probability distribution $P_L(T)$. Our key result is that the bulk of the distribution can be represented quite accurately by a Gaussian. The tails of course are not Gaussian since, among other reasons, T can vary only between 0 and 1.

In Fig. 4, we have plotted the four distributions for the four different values of $L=7, 8, 10,$ and 11 with $W=50$ as a function of the variable $X \equiv (T - \langle T \rangle) / \langle \Delta T^2 \rangle^{1/2}$. For comparison, the solid curve in this figure gives the Gaussian function $(2\pi)^{-1/2} \exp(-X^2/2)$. Note that there is *no* adjustable parameter and the agreement is

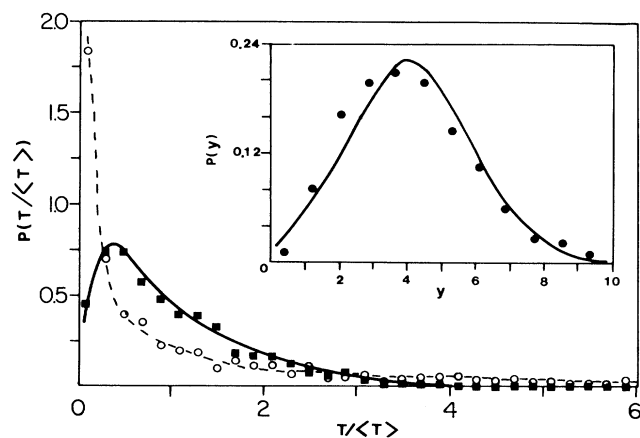


FIG. 5. Two distribution functions for $L=7$ and 15 with $W=5$. The symbols \blacksquare and \circ correspond to $L=7$ and 15 , respectively. The two curves are drawn through the calculated points to guide the eye. Note the long tail of the distribution for $L=15$. Inset: $P(y)$ as a function of y where $y = \ln T$ for $L=15$.

good.

We now turn to the case $L \gtrsim W$. When L increases for fixed W , one can expect a crossover from the diffusive regime discussed above to the regime of strong localization. In the crossover region, the relative fluctuation $\delta \equiv \langle \Delta T^2 \rangle / \langle T \rangle^2$ should be of order unity. Indeed, our calculations show that δ changes from 0.5 to 4.5 as L changes from 7 to 20 for $W=5$ and $|r|^2 = \frac{1}{4}$. In Fig. 5, we plot two distributions $P(T/\langle T \rangle)$ for two values of L for a fixed value of $W=5$ as a function of $T/\langle T \rangle$. The results clearly demonstrate that the distribution for $L=7$ (squares in Fig. 5) is entirely different from the case where $L=15$ (circles). The two curves are drawn through the calculated points to guide the eye. The distribution function for $L=15$ does not resemble a Gaussian-type shape (as was found in Fig. 4). Moreover, the long tail of the distribution demonstrates its major deviation from a Poisson-type distribution [as given by Eq. (4)] which is expected for quasi-one-dimensional systems only for *weak* disorder. Indeed, we find that $\langle T \rangle$ decreases with L faster than $1/L$ which indicates that we are close to strong localization. Correspondingly, we have plotted (see the inset of Fig. 5) the probability distribution $P(\ln T)$ for $L=15$ as a function of $\ln T$ and indeed find that it closely follows a Gaussian shape. The steady state was achieved after m_s steps (for $m > m_s$ the results did not change). For our smallest samples ($W=5$, $L=7$), $m_s \approx 150$ and for our largest samples ($W=50$, $L=15$), $m_s \approx 2000$.

In summary, we have developed a new numerical method for calculating interference phenomena. We have applied this method to one- and two-dimensional systems. In the one-dimensional case, the model yields results in agreement with analytical predictions. In the two-dimensional case, we have obtained new results for the probability distribution of the transmission which seems to be represented quite accurately by a Gaussian (*unlike* the one-dimensional case) as well as a crossover effect to log-normal behavior for the strong-disorder limit. We have also confirmed the diagrammatic results^{11,12} for $\langle \Delta T^2 \rangle$ in the weak-disorder limit.

This research was supported by the U.S.-Israel Binational Science Foundation and the Israel Academy of Sciences and Humanities.

¹For reviews, see G. Bergmann, Phys. Rep. **107**, 1 (1984); M. Pepper, Contemp. Phys. **26**, 257 (1985); P. A. Lee and T. V. Ramakrishnan, Rev. Mod. Phys. **57**, 287 (1985); N. F. Mott and M. Kaveh, Adv. Phys. **34**, 329 (1985).

²For a recent review, see S. John, Comments Condens. Matter Phys. (to be published).

³C. A. Condat and T. R. Kirkpatrick, Phys. Rev. Lett. **57**, 2725 (1987); S. John, H. Sompolinsky, and M. J. Stephen, Phys. Rev. B **27**, 5592 (1983).

⁴P. A. Lee and A. D. Stone, Phys. Rev. Lett. **55**, 1622 (1985).

⁵B. L. Altshuler and D. E. Khmel'nitskii, Pis'ma Zh. Eksp. Teor. Fiz. **42**, 291 (1985) [JETP Lett. **42**, 359 (1985)].

⁶Y. Imry, Europhys. Lett. **1**, 249 (1986).

⁷For a review, see S. Washburn and R. A. Webb, Adv. Phys. **35**, 375 (1986).

⁸Y. Imry, in *Directions in Condensed Matter Physics*, edited by G. Grinstein and G. Mazenko (World-Scientific, Singapore, 1986), p. 101; R. Landauer, in *Localization, Interactions and Transport Phenomena*, edited by B. Kramer, G. Bergmann, and Y. Bruynserade (Springer-Verlag, Heidelberg, 1985), p. 38.

⁹S. Etemad, R. Thompson, and M. J. Anderejco, Phys. Rev. Lett. **57**, 575 (1986); M. Kaveh, M. Rosenbluh, I. Edrei, and I. Freund, Phys. Rev. Lett. **57**, 2049 (1986).

¹⁰For earlier work on the effect of multiple scattering on distribution of intensity fluctuations, see V. I. Tatarskii, *Wave Propagation in a Turbulent Medium* (McGraw-Hill, New York, 1961); E. Jakeman and P. N. Pusey, Phys. Rev. Lett. **40**, 546 (1978); R. Dashen, Opt. Lett. **10**, 110 (1984); R. L. Phillips and L. C. Andrews, J. Opt. Soc. Am. **72**, 864 (1982). This work deals with fluctuations of the intensity at a *given* point whereas the present work calculates fluctuations of the transmission coefficient which is due [see M. J. Stephen and G. Cwilich, Phys. Rev. Lett. **59**, 285 (1987); S. Feng, C. Kane, P. A. Lee, and A. D. Stone, Phys. Rev. Lett. **61**, 834 (1988)] to *long-range* correlations between two *different* points.

¹¹Stephen and Cwilich, Ref. 10.

¹²Feng *et al.*, Ref. 10.

¹³This model for a stationary case was defined in B. Shapiro, Phys. Rev. Lett. **48**, 823 (1982) as a generalization of the model of P. W. Anderson, D. J. Thouless, E. Abrahams, and D. S. Fisher, Phys. Rev. B **22**, 3519 (1980).

¹⁴I. Edrei and M. Kaveh, Phys. Rev. B **38**, 950 (1988); I. Edrei and M. Kaveh, J. Phys. C **21**, L971 (1988).

¹⁵P. Mello, J. Math. Phys. **27**, 2876 (1986).

¹⁶B. Shapiro, Philos. Mag. **56**, 1031 (1987), and references therein.